

The design and construction of the MICE Electron-Muon Ranger

April 12, 2016

Abstract

The Electron-Muon Ranger (EMR) is a totally active scintillator detector installed in the beam of the Muon Ionization Cooling Experiment (MICE) [1]. The experiment will demonstrate ionization cooling, an essential technology needed for the realization of a Neutrino Factory and/or Muon Collider. The EMR is aimed at measuring the properties of the low energy beam composed of muons, electrons and pions, performing the identification particle by particle. The detector is made of 48 stacked layers alternately measuring the X- and the Y-coordinate. Each layer consists of 59 triangular scintillator bars. The read-out is based on FPGA custom made electronics and commercially available modules. This article will describe the construction of the detector, starting with the process of designing the detector up to its final commissioning with particle beam.

1 Introduction

The Neutrino Factory based on a high-energy muon storage-ring is the ultimate tool to study the neutrino mixing matrix and is established as the best facility to discover, and study the possible leptonic CP violation. It will produce the most intense, pure and focused neutrino beam ever achieved and is also the first step towards a $\mu^+\mu^-$ collider. The Neutrino Factory accelerator complex will use as a sources muons, produced as a tertiary beam. A proton beam bombarding a target will produce pions. These pions will be captured and focused in a high-field solenoid channel and will decay to muons, creating a low energy muon beam with very large emittance. The emittance of the muons needs to be reduced, i.e the muon must be “cooled”, so that the beam can be accelerated efficiently.

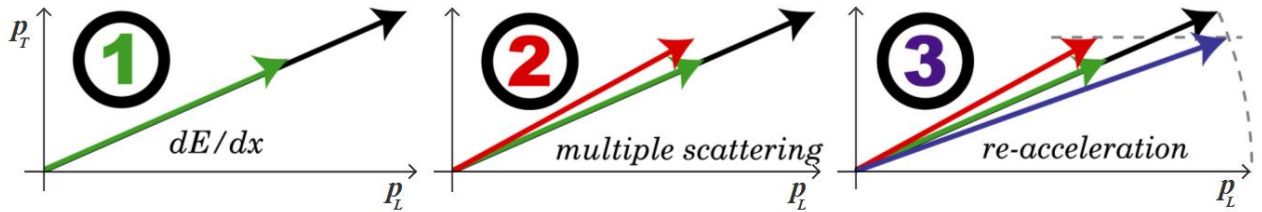


Figure 1: Ionization cooling principle: 1. Energy loss by ionization (dE/dx reduces P_L and P_T) 2. Heating from multiple scattering 3. P_L restored by RF cavities

Ionization cooling [2] (Fig. 1) provides the only practical solution to this problem, because it is fast enough to cool the beam within the muon lifetime ($\tau_\mu \sim 2.2 \mu s$). The cooling effect is accomplished by passing the muons through a low-Z material ("absorber"), in which they lose energy via ionization, reducing both the longitudinal and the transverse components of momentum. Later the longitudinal momentum is restored by accelerating cavities. The net effect is a reduction of the beam emittance. To maximize cooling we need the absorber to be placed at a position where the transverse momentum P_T has a maximum (the transverse betatron function β_\perp has a minimum).

1.1 MICE

The international Muon Ionization Cooling Experiment (MICE) [1] is under development at the Rutherford Appleton Laboratory (UK). The goal of the experiment is to build a section of a cooling channel that can demonstrate the principle of Ionization cooling and to verify its performance in a muon beam.

Since energy loss by ionization and multiple Coulomb scattering are momentum dependent, the ionization-cooling effect is momentum dependent. MICE (Fig. 2) uses variety of muon beams of limited intensity, having central momenta in the range $140 - 240 \text{ MeV}/c$ and a momentum spread of $\sim 20 \text{ MeV}/c$. These muon beams are generated using a titanium target [3] which is dipped into the ISIS proton beam [4]. Produced secondary and tertiary particles are captured, momentum-selected and transported to the cooling section by a system of magnets which includes: 5 T superconducting pion decay solenoid, two dipole magnets, nine quadrupole magnets and a mechanism for inflation of the initial emittance called Diffuser.

The cooling section of MICE, is similar to the cooling channel for the International Design Study for the Neutrino Factory [5]. It consists of one primary lithium-hydride (LiH) absorber, two secondary absorbers, two focus coils and two 201 MHz RF cavities. The two superconducting focus-coil modules provide strong focusing at the absorber, ensuring that the transverse betatron function is minimised at this position and enhancing the cooling effect. All beam particles are detected individually by two identical Scintillating fiber trackers in 4T solenoids, situated upstream and downstream of the cooling section. The beam emittance is reconstructed, by measuring the spatial coordinates and momentum (x, y, p_x, p_y, p_z) of each muon.

The particle content of the beam is measured by a dedicated system of detectors situated upstream and downstream of the cooling section and designed to provide precise muon, pion and electron identification. The upstream part includes two Time-of-flight hodoscopes (TOF0 and TOF1) and a Cherenkov detectors (CKOV). The downstream part combines another Time-of-flight hodoscope (TOF2) and a calorimeter system. The calorimeter system consists of the KLOE-Light (KL) lead-scintillator sampling calorimeter, similar to the KLOE design [30], but with thinner lead foils, serving as a preshower for the totally-active Electron-Muon ranger (EMR), situated behind him.

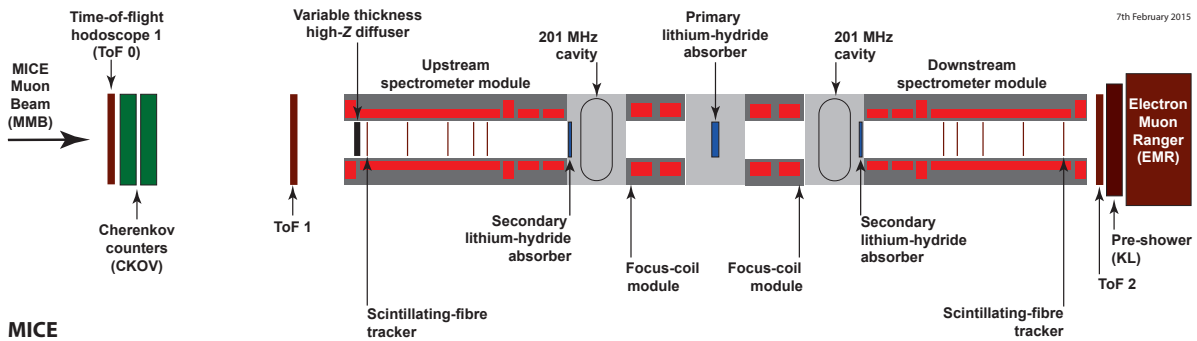


Figure 2: Schematic view of the MICE experiment.

MICE will measure the normalised transverse emittance ϵ_N with a precision of $\sigma_{\epsilon_N}/\epsilon_N \sim 0.1\%$ when 6% cooling effect is expected for a muon beam with a nominal momentum of $200 \text{ MeV}/c$ and 4D normalised emittance $\epsilon_N = 5.8 \pi mm \times rad$ is .

2 Electron-Muon Ranger (EMR)

EMR is a fully active scintillator detector. It can be classified as tracking calorimeter, since its granularity allows for track reconstruction. The primary purpose of the detector is to distinguish muons from their decay products, rejecting events in which the muon decays in-flight along the cooling section [6]. This allows for the selection of a muon beam with a contamination below 1%. The range of the muon track can be measured, providing an estimate of the momentum of the muon.

The construction of the detector started in the early 2011 and in October 2013 the detector was fully commissioned with beam during one month of a dedicated data-taking at RAL. In 2014 the detector was upgraded, including a replacement of the single-anode photo-multiplier tubes and installation of a new high-voltage system.

2.1 Design

The EMR is built of triangular scintillator bars arranged in planes. One plane contains 59 bars and covers an area of 1.27 m². Each even bar is rotated by 180 degrees with respect to the odd one. A cross-section of bars and their arrangement in a plane is shown in Figure 3. With this configuration there is no dead area for particles crossing a plane with angles less than 45 degrees from the beam axis.

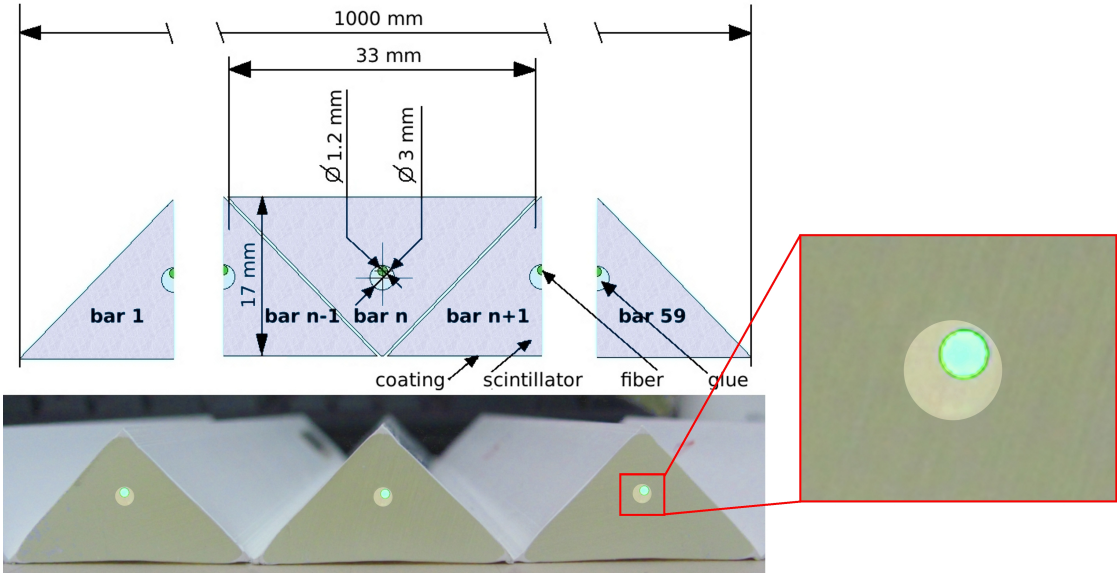


Figure 3: EMR bar cross-section and bars arrangement in a plane. There are 59 bars per plane.

The light, produced when a particle crosses a bar, is collected by a wave-length shifting (WLS) fiber glued inside the bar. Transparent epoxy¹ is used to glue the WLS fiber in order to increase the light collection efficiency. At both ends of a bar the WLS fiber is coupled to a clear fiber that transfers the light to a photo-multiplier (PMT). The clear fibers are protected with rubber sleeves and packed in aluminum fiber boxes as drawn in Figure 4. In order to reduce the bending radius, which affects light attenuation, each fiber has individual length. The two bunches of clear fibers coming from the two sides of a plane are glued into different types of connectors. One is designed to match a multi-anode PMT, when the other one matches a single-anode PMT.

¹Prochima E30 water effect resin

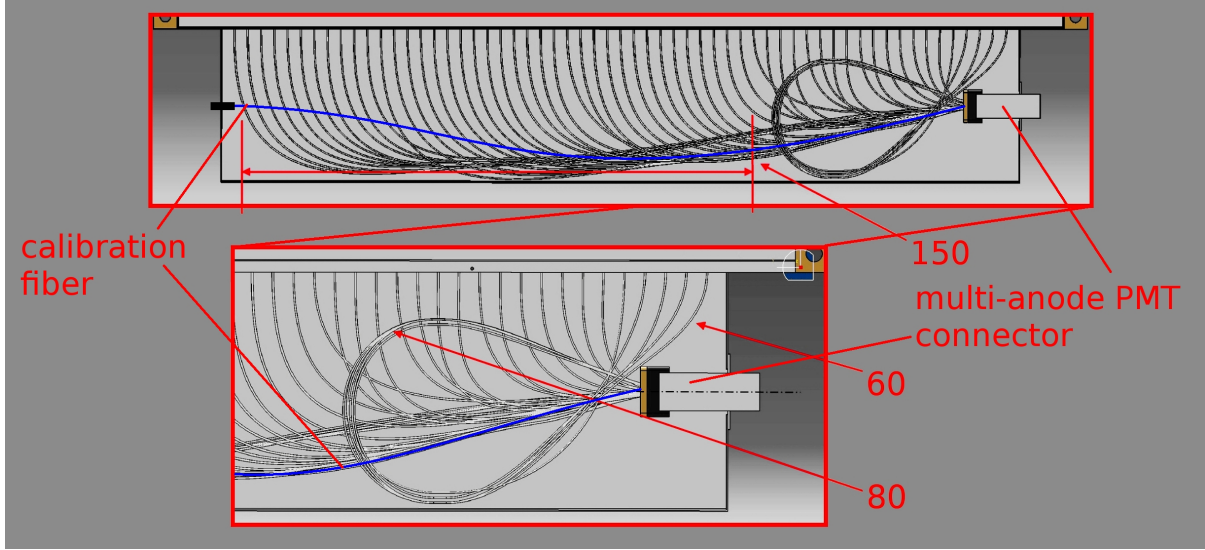


Figure 4: A package of clear fibers in a fiber box. Multi-anode PMT connector is shown. The fiber box for single-anode PMT connector has similar structure. The last 5 fibers are looped in order to have largest possible bending radius. The bending radius of some of the fibers is indicate in red. The calibration fiber is also shown.

Two planes attached to each other via aluminum profiles form a rigid structure called module (Figure 5). The full detector contains 24 modules as shown in Figure 6. Panels cover all sides of the detector in order to insure a light-tightness. The signal coming from each multi-anode PMT is read-out and processed by a front-end board attached directly to the fiber box as shown in Figure 5. The single anode PMTs is equipped whit a voltage divider and the analog signal is sent outside the detector for digitization.

A calibration system was installed inside the enclosure of the detector in order to monitor the drift of the gain and the quantum efficiency of the PMTs. This system is made of a LED driver distributing light homogeneously to 100 fiber. Each fiber box is connected to one of the calibration fibers through a dedicated connector. Inside a fiber box a clear fiber connects the calibration fiber to the PMT.

All cables inside the detector are feed through four patch-panels. There are 96 high-voltage, 6 low voltage, 48 analog, 48 digital, and one configuration cables in total. A support frame is designed to withhold the full weight of the sensitive volume with electronics (~ 1 tonne). In order to protect the front-end electronics from the magnetic field of the spectrometer solenoid, situated nearby the detector, a shielding plate is mounted on the side of the detector that faces the beam. The total weight of the detector is almost 2.5 tonnes.

2.2 Optical Elements

The scintillator bars were manufactured at extrusion facility at Fermilab [7]. This facility also produced scintillators of different shapes for other experiments like: DO preshower detector, MINOS [8], Minerva [9], SciBar (K2K/SciBoone), Star, Mayn Pyramid Mapping, Hall-B JLAB, T2K-ND280, Double-Chooz, Amiga - Pierre Auger. Each bars is 110 cm long, 1.7 cm high and 3.3 cm wide with 3 mm hole along the bar for a wavelength shifting fiber. The scintillator is made of polystyrene

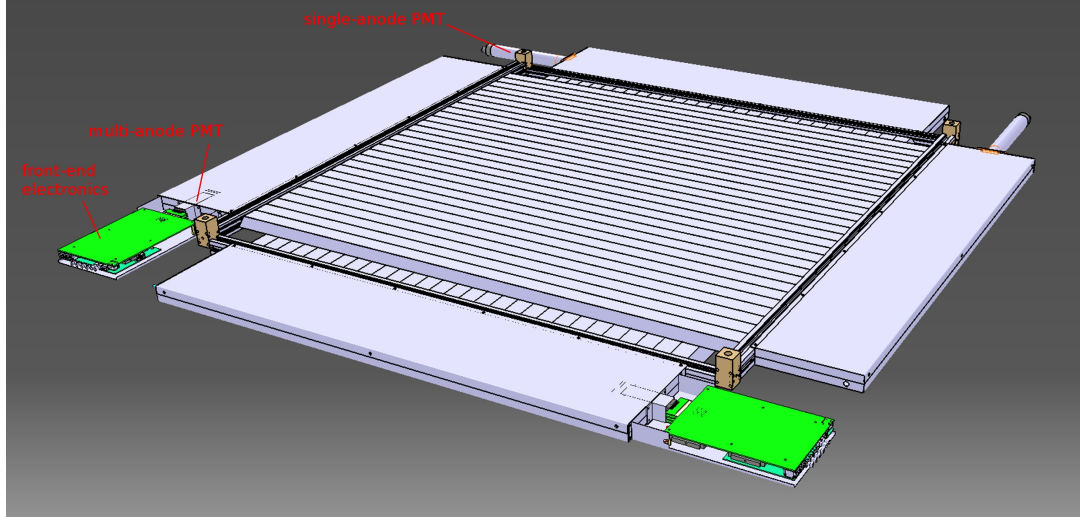


Figure 5: CAD drawing of one EMR module made of X and Y planes. There are two front-end boards per module.

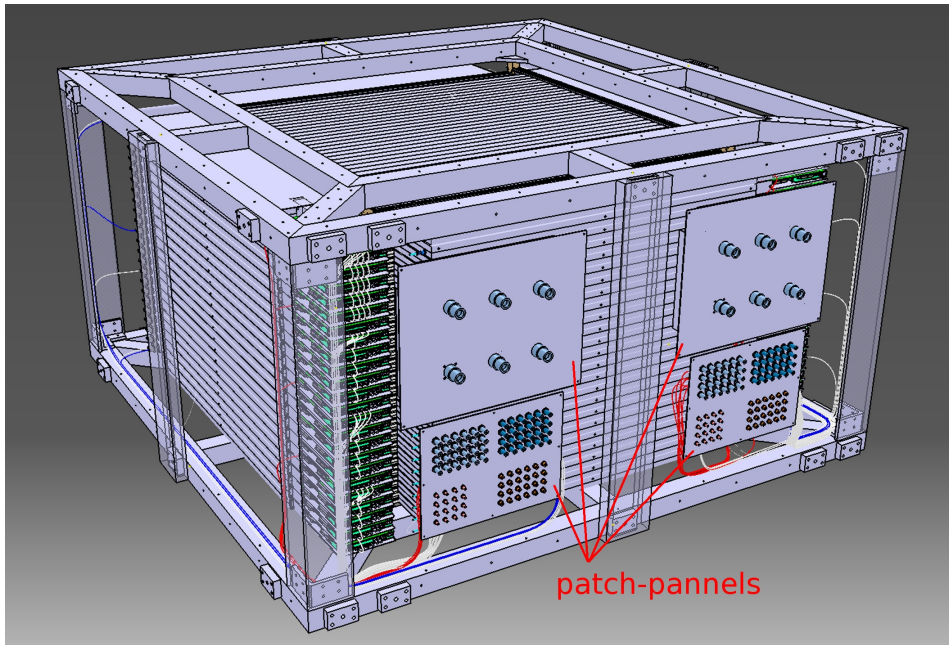


Figure 6: CAD drawing of the complete EMR detector. The external protective panels are not shown.

pellets² as base, 1% PPO³ as primary and 0.03% POPOP⁴ as secondary fluor. Each bar is coated with TiO₂ reflector to increase light collection by a wavelength shifting fiber inserted inside the scintillator. Light output of the scintillator was measured [7] with a photo-multiplier (25% quantum efficiency) and it is around 17 photo-electrons.

The WLS fiber glued inside the bar is a double cladding 1.2 mm in diameter fiber, produced by

²Dow Styron 663 W

³scintillator, 2,5-diphenyloxazole, C₁₅H₁₁NO

⁴wavelength shifter, 1,4-di-(5-phenyl-2-oxazolyl)-benzene, C₂₄H₁₆N₂O, spectrum peaks at 410 nm (violet)

Saint-Gobain Crystals [10]. The core material of the fiber is polystyrene with acrylic cladding. It has very large numerical aperture of 0.58 compared to 0.2-0.3 of graded-index multimode fiber used in data communications. Trapping efficiency is 3.5%. The light is absorbed in blue part of a visible spectrum and re-emitted in green.

The clear fiber, used to transfer light from the ends of scintillator bar to the PMTs, is a 1.5mm multi-cladding fiber produced by Kuraray [11] with special structure (S-type) that allows for better rigidity against bending. The aperture of this fiber matches to the one of WLS fiber so that insertion loss is minimal.

A special connector was designed to couple a clear fiber to a wavelength shifting fiber (see Figure 7). It has a small cylindrical enlargement which is meant to be filled with glue to fix the fiber in the connector. Thanks to that configuration it is possible to avoid crimping the fiber since a sharp edge of the connector would easily damage it. As shown in Figure 7 the retaining clip (B) is screwed into the wavelength shifting fiber connector (A) so that clear fiber connector can be easily and safely attached. All these pieces are non-standard and could not be found on a market, therefore a special mold was designed to produce them using injection molding technique.

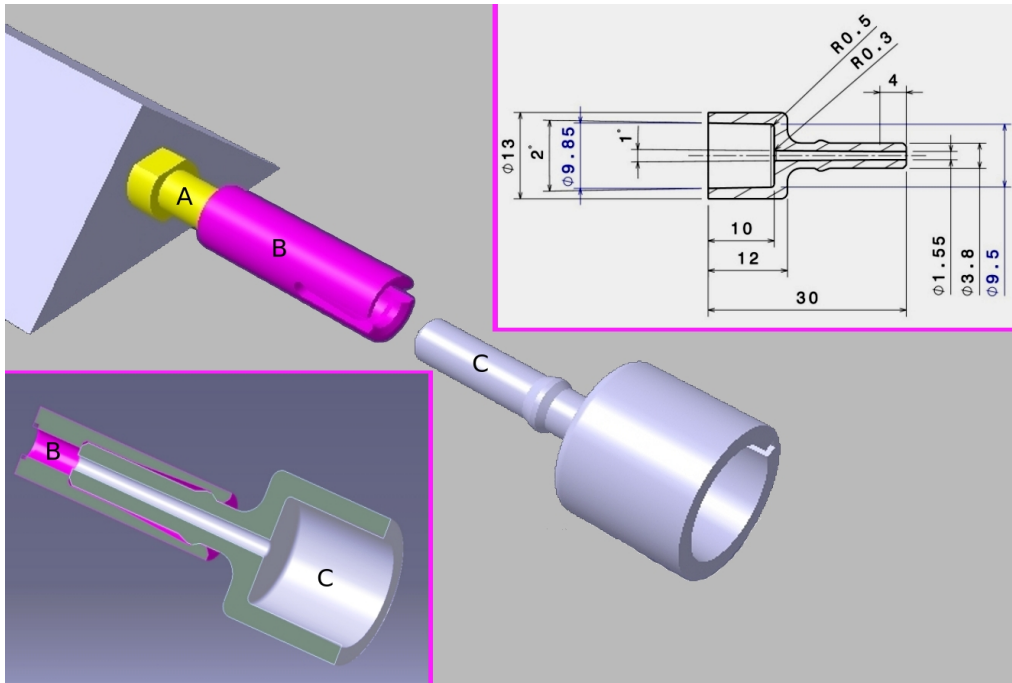


Figure 7: clear fiber connector (C) is attached to the wavelength shifting fiber connector (A) via retaining clip (B).

Both faces of the bar's fiber connectors are polished with a special polishing machine. Four different grades of sand paper are used to achieve a mirror like quality of the polished surfaces. The last step is performed using a $1\mu\text{m}$ grade diamond-based polishing paper. The same procedure is applied to the clear fiber connectors and PMT connectors (see Figure 8).

2.3 Photodetectors

As it was briefly mentioned earlier the EMR has a dual readout. Each scintillator plane is equipped with a multi-anode PMT, which collects the light from the individual bars and a single-anode PMT which detects the integrated response of all bars.

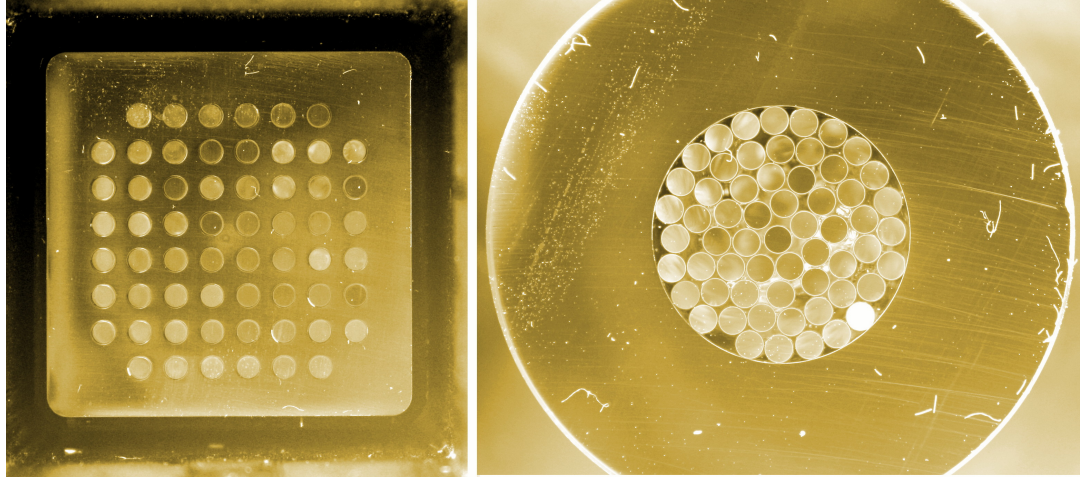


Figure 8: **Left:** multi-anode PMT connector. **Right:** single-anode PMT connector.

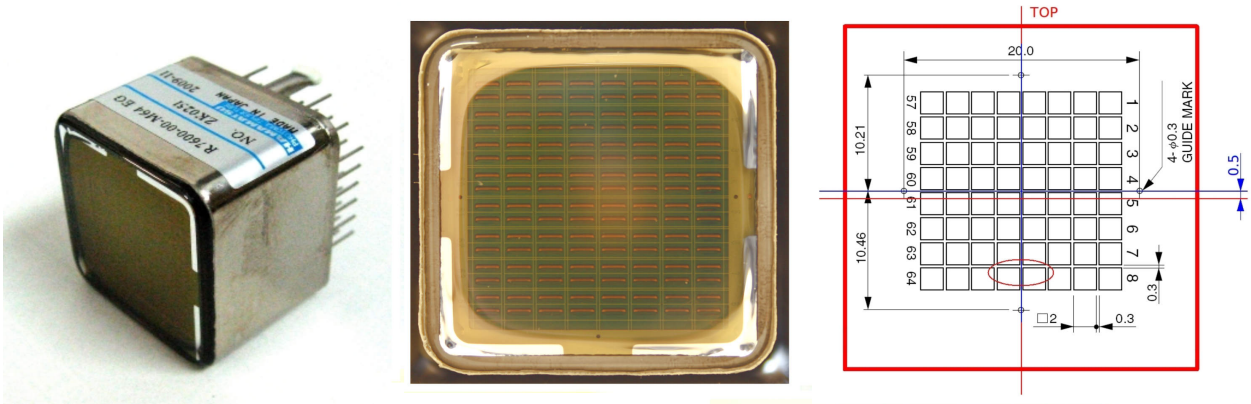


Figure 9: Multi-Anode PMT. **Left:** photo. **Center:** anode matrix. **Right:** anode matrix dimensions.

The multi-anode photo-multiplier tube (MAPMT) is a 64-channel PMT produced by Hamamatsu (model R5900-00-M64 [12], see Figure 9, left). The spectral sensitivity matches to the emission spectrum of the wavelength shifting fiber. It is placed in a μ -metal tube which serves as additional shielding against the static magnetic field. Inside μ -metal tube, the PMT is aligned with respect to the fiber connector in such a way that each fiber shines only one channel. Therefore it was important to measure all dimensions of the PMT and especially position of the anode matrix with respect to the PMT case (Figure 9, centre). Figure 10 shows distributions of the measured dimensions (width and height) and displacements of the anode matrix for 53 MAPMTs. It was found that on average the matrix is shifted by 0.5 mm upwards (see Figure 9, right and Figure 10, bottom right). This was taken into account in the design of the MAPMT fiber connectors.

As for the MAPMTs, the single-anode photo-multiplier tube (SAPMT) is placed in a μ -metal tube. The EMR detector was initially assembled by reusing old SAPMTs, available after the disassembly of the HARP experiment [13]. These were 10 stage linear focused PMTs produced by Philips (model XP2972). A special selection procedure was developed in order to select the best samples for the assembly of the detector [14]. In 2014, during the upgrade of the detector, all Philips SAPMT were replaced by new SAPMTs produced by Hamamatsu (model R6427 [12]).

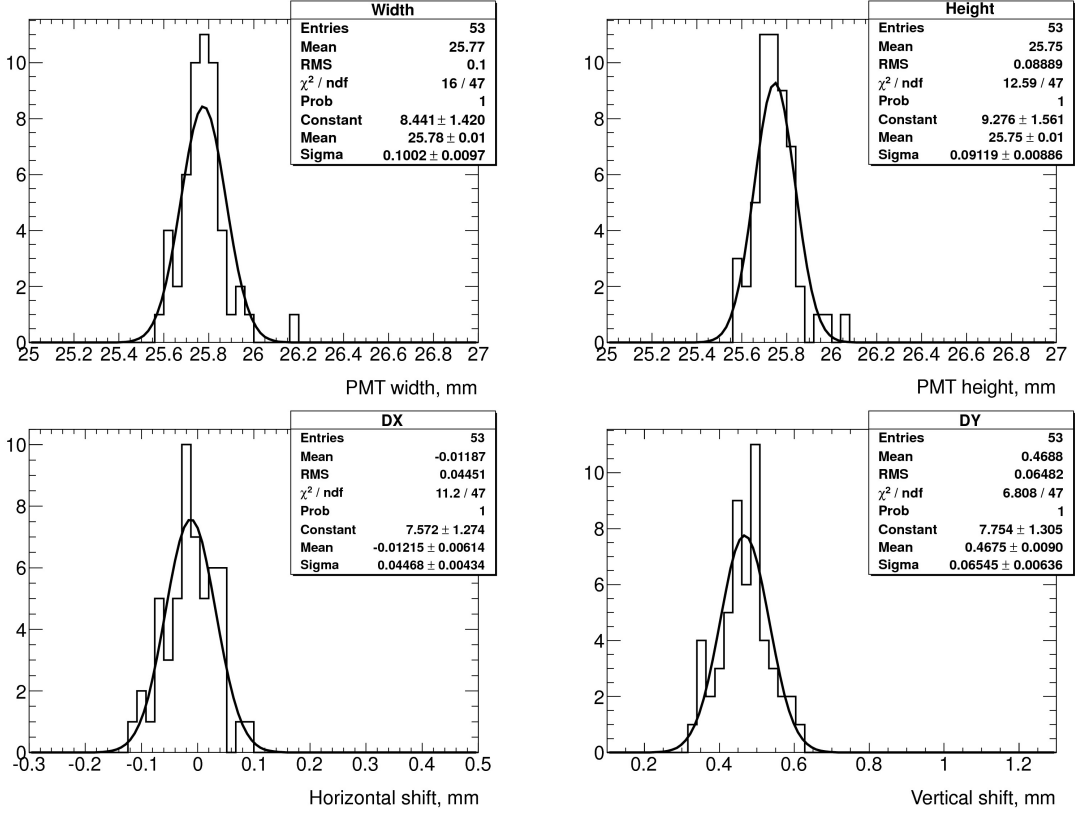


Figure 10: Distribution of Multi-Anode PMT dimensions.

2.4 Electronics Layout

In MICE the spill is defined as the period when the target crosses the ISIS proton beam. The maximum spill repeating rate allowed by the MICE target system is $\sim 0.75 \text{ Hz}$. The overall principle of the MICE Data Acquisition (DAQ) system is that during the spill the accumulated digital data is kept in local memory buffers and the readout is performed only at the end of the spill.

A schematic layout of the EMR electronics is shown in Figure 11. The multi-anode PMT connected via a flex cable to a front-end board which processes the signal and sends it to a piggy-back buffer board for digitization and storage. The front-end board is configured by the VME configuration board, which resides in the VME crate in the control rack. This board is able to configure up to 16 front-end boards, therefore three of them are required for the full detector. The buffer boards are readout by groups of six. In each group the first buffer board is a master and other five are slaves. All six boards are daisy-chained via ethernet cable and the master is connected to a VME readout board, which transfers all the data from the six buffer boards to the DAQ computer. In the whole detector there are 8 groups of buffer boards, i.e. 8 VME readout boards are installed in the control rack.

2.4.1 Front-End and Buffer Boards

The multi-anode PMT is readout by a dedicated front-end board equipped with piggy-back buffer board which stores hit information during a spill. Figure 12 show the full assembly that is mounted on every plane of the detector. It consists of a PMT attached to a voltage divider which is connected to the front-end board through a flex cable. This cable also creates additional pressure between the

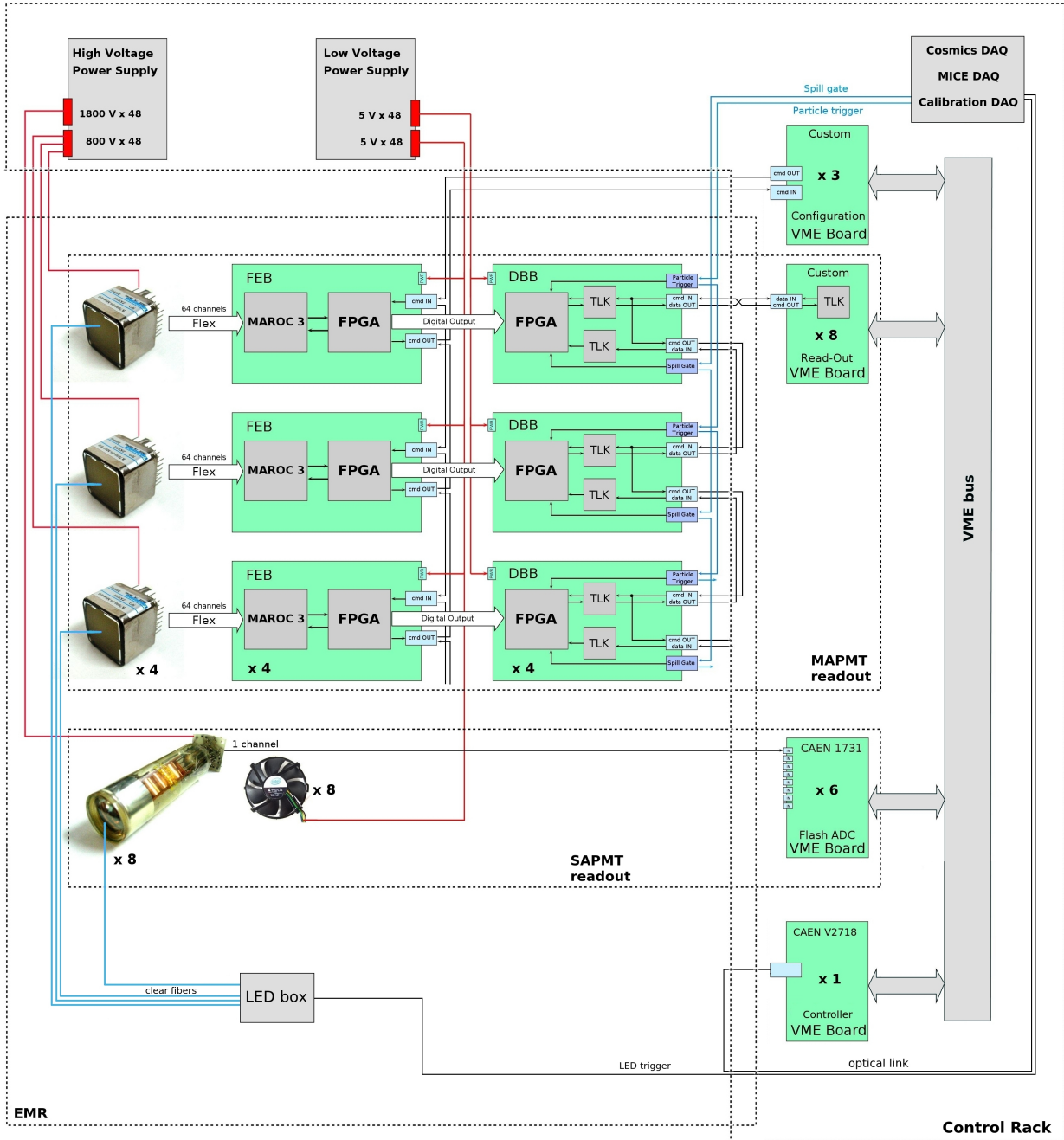


Figure 11: EMR electronics layout. **FEB:** front-end board for multi-anode PMT readout. **DBB:** buffer board. **MAROC 3:** 64 channel readout ASIC for multi-anode PMT. **MAPMT:** multi-anode PMT. **SAPMT:** single-anode PMT.

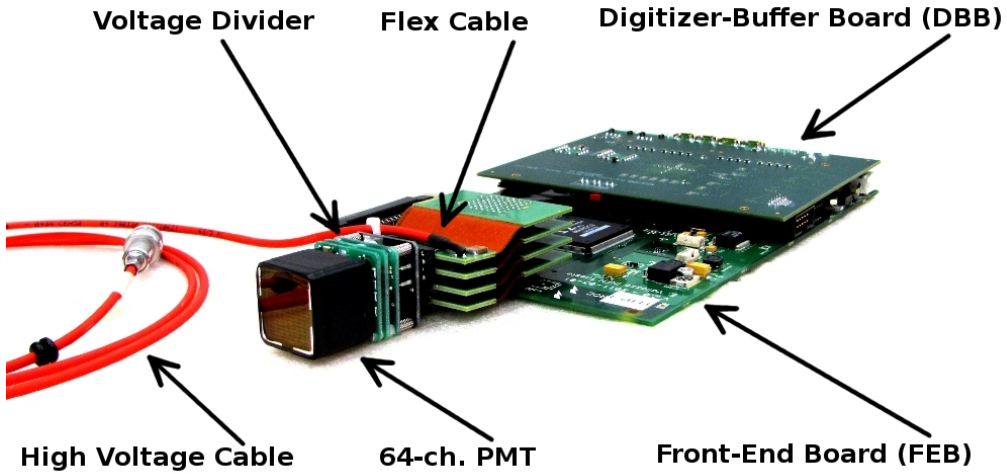


Figure 12: Front-end and buffer board assembly.

PMT and fiber connector. The front-end board is able to process all 64^5 signals of the MAPMT thanks to 64-channel ASIC⁶ called MAROC⁷. The 64 analog signals are feed into the MAROC chip where they are shaped and discriminated. The discriminated signals are then forwarded to two high density connectors where buffer board is connected. The width of the discriminated signal represents time over threshold measurement. The MAROC ASIC also provides analog measurement - signal charge. This measurement is based on a slow shaper and is multiplexed from all the channels and it requires a trigger (either external or internal) to produce a measurement. It takes tens of microseconds (depending on MAROC configuration) to process all the multiplexed signals and this dead time is not acceptable for the MICE DAQ duty cycle (a few hundred triggers per 1 ms spill). Therefore only time-over-threshold measurement is used since it is practically dead-timeless. The function of the FPGA chip⁸ is mainly to forward data from MAROC to the buffer board and to send configuration signals from the VME configuration board to the MAROC and verify their status. The board has separate power for analog and digital part (both 5 V). The total power consumption of the board is 0.6 Amp.

The two essential roles of the buffer board are to sample the 63 channels (and external trigger) coming from the front-end board and to transmit the event data upon request of the acquisition system. The digitization starts when the board receives the Spill Gate signal from an external LEMO connector. The number of clock ticks from the beginning of the spill to the leading edge and trailing edge of every discriminated signal coming from the front-end board is recorded. The difference between the two measurements represents the time over threshold of the original signal. The clock sampling rate is 400 MHz (2.5 ns resolution). An external trigger is also recorded by the buffer board. The trigger signal is feed into one of the 64 input channel and is treated as any other signal. Therefore, only 63 channels are recorded from the front-end board. The board also calculates the width of every spill, counts the number of spills, number of triggers in the spills, and number of hits in every channel.

The general architecture of the DBB is organized around a single FPGA⁹ that performs the

⁵Each EMR plane contains 59 scintillator bars which results in having 5 redundant channels.

⁶Application-Specific Integrated Circuit

⁷Multi Anode ReadOut Chip

⁸Altera Cyclone II (EP2C35F484C8N)

⁹Altera Stratix II (EP2S30F484C3N)

sampling, data buffering, and dataflow control functions of the board. Internal memory of the FPGA, configured as FIFO, is used to store the event data which is a collection of leading and trailing edge timestamps that occurred on each channel during a specific spill. Two gigabit transceivers¹⁰ are interfaced to the FPGA to provide the physical transmission channels and form an upstream command link and a downstream data link. Six DBB's are grouped together and daisy-chained with upstream and downstream links via ethernet cable. The first DBB in each group is directly connected to the acquisition system - the VME readout board - via four coaxial cables.

2.4.2 Configuration Board

The VME configuration board is a single FPGA¹¹ board designed to perform configuration of the MAROC chip on the front-end board. The communication between the boards is realized via LVDS¹² signals driven and received by LVDS drivers/receivers directly connected to corresponding FPGA's. As mentioned in the previous section, it can read analog signal (charge of the signal from every channel) from the front-end board but it is not implemented in the current design. The board is connected to VME bus through which it communicates with the VME controller and the DAQ computer. The MAROC chip is configured by TTL¹³ signal composed of 830 bits which code the configuration parameters.

2.5 VME Read-Out Board

One VME readout board performs the readout of one group of six buffer boards. It is a single FPGA¹⁴ board with a gigabit transceiver¹⁵ which drives the signals to and from the buffer boards. During the readout cycle the board should store the data from 6 buffer boards, therefore it is equipped with four high-speed 16M-bit static RAMs¹⁶ each organized as 1024K words by 16 bits. It communicates with the DAQ computer via VME bus through the VME controller. Additional LVDS input/output connector is available but not used.

2.6 Fast ADC Board

The Flash ADC Waveform Digitizer made by CAEN [15] is used to readout signals from single-anode PMTs. The ADC has a sampling frequency of 500 M samples per second (2 ns resolution timing resolution). A pulse shape of each input signal is digitized by 8 bit ADC and continuously written in a circular memory buffer. When a trigger arrives the FPGA writes certain number samples defined by the pre- and post-trigger settings into a buffer which then is available for readout via VME bus.

¹⁰TLK1501

¹¹Altera Cyclone II (EP2C50F484C8N)

¹²Low-Voltage Differential Signaling, communication protocol.

¹³Transistor-Transistor Logic

¹⁴Altera Cyclone II (EP2C50F484C8N)

¹⁵TLK1501

¹⁶IS61WV102416BLL-10TLI - SRAM, 16Mb, 10ns, 48TSOP

References

- [1] Mice web site. <http://mice.iit.edu>, contains detailed information about the experiment.
- [2] D. Neuffer. Principles and applications of muon cooling. *Part. Accel.*, 14:75, 1983.
- [3] C. N. Booth and et al. The design, construction and performance of the mice target. *Journal of Instrumentation*, 8:P03006, 2013.
- [4] ISIS pulsed neutron and muon source at the Rutherford Appleton laboratory. web site. <http://www.isis.stfc.ac.uk>.
- [5] S. Choubey et al. International design study for the neutrino factory. *Interim Design Report*, IDS-NF-20, 2011. arXiv:hep-ex/1112.2853.
- [6] R. Asfandiyarov. Totally active scintillator tracker-calorimeter for the Muon Ionization Cooling Experiment. *University of Geneva, PhD thesis*, 2014.
- [7] A. Pla-Dalmau, A. Bross, and K. Mellott. Low-cost extruded plastic scintillator. *Nucl. Instrum. Meth.*, A466:482–491, 2001. FERMILAB-PUB-00-177-E.
- [8] A. Pla-Dalmau. Extruded plastic scintillator for the MINOS calorimeters. *Frascati Phys.Ser.*, 21:513–522, 2001. FERMILAB-CONF-00-343.
- [9] A. Pla-Dalmau, A. Bross, V. Rykalin, and B. Wood. Extruded plastic scintillator for MINERvA. *Nuclear Science Symposium Conference Record, IEEE*, 3, 2005. FERMILAB-CONF-05-506-E.
- [10] Saint-Gobain Crystals. Scintillating fiber brochure.
- [11] Kuraray. Plastic scintillating fibers brochure.
- [12] Hamamatsu. Multianode photo-multiplier tubes R5900-00-M64 datashee.
- [13] M. G. Catanesi et al. [HARP Collaboration]. The HARP detector at the CERN PS. *Nucl. Instr. and Meth.*, (A 571):527, 2007.
- [14] R. Asfandiyarov et al. Selecting philips xp 2972 photomultiplier tubes for the electron muon ranger (emr). *MICE internal note*, 2012. MICE-NOTE-DET-383.
- [15] CAEN. V1731 4/8 ch. 8 bit 1000/500 ms/s Digitizer. Technical information manual.